Original Paper

phys. stat. sol. (b) **242**, No. 10, 2041–2050 (2005) / **DOI** 10.1002/pssb.200540069

First-principles calculations of the CaF_2 bulk and surface electronic structure

H. Shi, R. I. Eglitis*, and **G. Borstel**

Universität Osnabrück, Fachbereich Physik, 49069 Osnabrück, Germany

Received 6 January 2005, revised 8 April 2005, accepted 24 May 2005
Published online 7 July 2005

PACS 68.35.Bs, 71.15.Ap, 71.15.Mb, 71.20.Ps, 73.20.At

We present and discuss the results of calculations of the CaF_2 bulk and surface electronic structure. These are based on the *ab initio* Hartree–Fock (HF) method with electron correlation corrections and on Density Functional Theory (DFT) calculations with different exchange-correlation functionals, including hybrid exchange techniques. Both approaches use the localised Gaussian-type basis set. According to our calculations the *ab initio* HF method considerably overestimates (20.77 eV) the optical band gap, whereas the density functional calculations based on the Kohn–Sham equation with a number of exchange-correlation functionals, including local density approximation (LDA) (8.72 eV), generalized gradient approximations (GGA) by Perdew and Wang (PW) (8.51 eV), and Perdew, Burke, and Ernzerhof (PBE) (8.45 eV) underestimate it. Our results show that the best agreement with experiment (12.1 eV) can be obtained using a hybrid HF–DFT exchange functional, in which Hartree–Fock exchange is mixed with DFT exchange functionals, using Beckes three parameter method, combined with the non-local correlation functionals by Perdew and Wang (B3PW) (10.96 eV). We also present calculations of CaF_2(111), (110), and (100) surfaces. Our calculated surface energies using the hybrid B3PW method confirm that the CaF_2(111) surface is the most stable one, in agreement with the experiment.

1 Introduction

Considering the high technological importance of CaF_2, it is not surprising, that during the last years, it has been the subject of many experimental and theoretical studies [1–11]. Fluorite CaF_2 is a cubic $Fm3m$ large gap insulator. The unit cell includes three ions, one cation chosen as origin, and two anions which are situated at (1/4a, 1/4a, 1/4a) and (3/4a, 3/4a, 3/4a), where a is the lattice constant. The experimental lattice constant for CaF_2 is 5.4630 Å [12]. To date, a large amount of experimental information on CaF_2 has been accumulated [3, 13–15], which requires an interpretation from the stand point of the band structure of this crystal. Experimentally, the direct band gap is 12.1 eV [1] and the indirect gap is estimated to be 11.8 eV [2].

The electronic structure of CaF_2 has been recently calculated from first principles and published by several research groups. In the beginning of the Nineties M. Catti et al. [6] performed an all-electron *ab initio* HF calculation for the band structure of CaF_2. The energy gap-width between valence and conduction bands at the Γ point was about 21 eV, considerably exceeding the experimental value.

From another side, it is well known that the local-density and generalized-gradient approximations to DFT systematically underestimate the band gap in semiconductors and insulators: An error of a factor 2 is typical. For example, in Ref. [1] the indirect band gap ($X \rightarrow \Gamma$) of 7.07 eV is underestimated with respect to experiment as expected in a GGA-DFT calculation. A similar result for the indirect band gap

* Corresponding author: e-mail: reglitis@uos.de, Phone: +49-541-9692667, Fax: +49-541-9692351

in CaF_2 (6.53 eV) using the first-principles orthogonalized linear combination of atomic orbitals (OLCAO) method in the local-density approximation (LDA) was obtained by F. Gan et al. [4].

We calculated the electronic structure of bulk CaF_2 by means of *ab initio* calculations based on Hartree–Fock (HF) and density functional theory (DFT) methods. It turns out that results obtained by hybrid exchange technique (B3PW) are in best agreement with available experimental data. We also present in a second part of the paper theoretical investigations for pure CaF_2(111), (110) and (100) surfaces.

2 Method of calculations

All numerical calculations dealing with the CaF_2 electronic structure were performed by the CRYSTAL-2003 computer code [16]. In our calculations we used several quite different methods: Hartree–Fock with different density functional theory (DFT) type a posteriori electron correlation corrections to the total energy [17] such as generalized gradient approximation (HFGGA), Perdew-91 (HFPer91), Lee–Yang–Parr (HFLYP), and full scale DFT calculations based on the Kohn–Sham equations with a number of exchange-correlation functionals, including local density approximation (LDA), (GGA) by Perdew and Wang (PW), Perdew, Burke and Ernzerhof (PBE), as well as Becke exchange functionals using Beckes three-parameter method, combined with the non-local correlation functionals by Perdew and Wang (B3PW), as those by Lee, Yang and Parr (B3LYP). The CRYSTAL-2003 code uses the localized Gaussian-type basis set. In our calculations for CaF_2 we applied the all electron basis set developed by M. Catti et al. [6] and used a modified conjugate gradient algorithm [18, 19] to optimize the atomic coordinates and locate minima on the potential energy surface (PES).

We performed band structure calculations with $8 \times 8 \times 8 = 512$ k-points in the Brillouin zone (BZ). The calculated thresholds N (i.e., the calculation of integrals with an accuracy of 10^{-N}) were chosen as a compromise between the accuracy of the calculations and the large computational time for large cells. They are 7, 8, 7, 7, and 14 for the Coulomb overlap, Coulomb penetration, exchange overlap, the first exchange pseudo-overlap, and for the second exchange pseudo-overlap, respectively [20]. The convergence criteria for the Self Consistent Field (SCF) energy and eigenvalues were set to 10^{-10} and 10^{-12} a.u., respectively.

3 Results of calculations

3.1 CaF_2 bulk electronic structure

As a starting point of our calculations, we have tested how different methods reproduce the experimentally observable bulk properties – lattice constant a_0 and the bulk modulus B. The LDA calculations underestimate a_0 by 2.2% and overestimate B by 24.5%. The HF method without any correlation corrections to the total energy overestimates both a_0 (by 1.1%) and B (by 12.4%). HF with GGA corrections overestimates a_0 by 0.9% and B by 6.4%. Lastly, the hybrid B3PW method gives the best result for the lattice constant a_0 (overestimates only by 0.7%) and also for B (overestimates by 2.7%) (see Table 1).

Table 2 presents results for the effective atomic charges and bond populations. The effective charges for Ca and F ions, both in the bulk and on the surface, turn out to be only slightly smaller than the formal ionic charges (+2e and –e, respectively). This arises due to the high ionic nature of the Ca–F chemical bonding. Note that these results are close for all methods used. The most obvious difference is between the effective charges for the Ca ion calculated by LDA (+1.728e) and HF (+1.895e). Obviously, there is practically no chemical bonding between Ca–F or F–F, since the relevant bond populations are even

Table 1 Optimized lattice constant a_0 (Å), and bulk modulus B (GPa) for CaF_2.

method	LDA	PWGGA	PBE	BLYP	B3PW	B3LYP	HF	exp.
a_0 (Å)	5.34	5.51	5.52	5.56	5.50	5.52	5.52	5.46
B (GPa)	103	88	90	79	85	91	93	82.71

Table 2 Static (Mulliken) charges of atoms and bond populations (in *me*) for bulk CaF_2 calculated by various methods.

atom	charge Q (e) bond pop. P (*me*)	LDA	PWGGA	PBE	BLYP	B3PW	B3LYP	HF
Ca^{2+}	Q	+1.728	+1.769	+1.771	+1.776	+1.803	+1.805	+1.895
F^-	Q	–0.864	–0.885	–0.886	–0.888	–0.902	–0.903	–0.948
F–Ca	P	–28	–8	–6	–8	–10	–12	–18
F–F	P	–38	–20	–18	–18	–22	–22	–24

negative. Figure 1 shows the charge density map of CaF_2 bulk from the (110) side view obtained with the B3PW method. Figure 1 confirms that the charge density between atoms is very small in agreement with the charge and bond population calculations, reflecting the high degree of ionic bonding in this crystal.

Experimentally, the direct band gap for CaF_2 bulk is 12.1 eV [1] and the indirect band gap is estimated to be 11.8 eV [2]. It is well-known fact that DFT-LDA calculations underestimate the band gap by a factor of typically two. According to our calculations, the indirect band gap ($X \rightarrow \Gamma$) using the LDA to the density functional theory is 8.44 eV (see Table 3), considerably less as obtained experimentally.

On the other hand, the band gap obtained through pure-HF calculations usually greatly overestimates the experimental value [20]. Indeed, results of our pure HF calculations for indirect band gap ($X \rightarrow \Gamma$) (20.43 eV) confirms this rule (see Table 3). A possible solution of this problem is the use of so-called *hybrid* functionals (a combination of the non-local HF exchange, DFT exchange, and the generalized gradient approximation (GGA) correlation functional). Examples are so-called B3PW and B3LYP which nowdays are extremely popular in quantum chemistry of molecules and recently have been applied to periodic-structure *ab initio* calculations of a wide range of crystalline materials [21], including perovskites and their surfaces [22–24]. Also in our case, for the CaF_2 bulk electronic structure, the hybrid B3PW and B3LYP methods gives the best results (see Table 3). Namely, according to our calculations, the indirect band gap ($X \rightarrow \Gamma$) using B3PW is 10.68 eV (see Fig. 2) and 10.57 eV by the B3LYP functional.

The upper valence band consists of F p-orbitals, whereas the conduction band bottom consists essentially of Ca d-orbitals. The orbital contribution from F atoms is small in this energy range (see Fig. 3).

3.2 Atomic and electronic structure of CaF_2 (111), (110) and (100) surfaces

Firstly, we determined the displacements of the atomic coordinates in several planes near the surface, where we calculate the effective atomic cahrges and bond populations between nearest atoms in order to characterize the chemical bonding. We started our calculations from the case of CaF_2(111) surface, which is known to be experimentally stable. Results of geometry optimization for 9 layers of CaF_2(111)

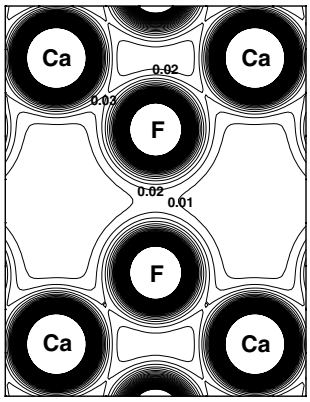

Fig. 1 (online colour at: www.pss-b.com) Charge density map of CaF_2 bulk from (110) side view calculated by means of hybrid B3PW method. Isodensity curves are drawn from 0 e/Bohr^3 to 0.5 e/Bohr^3 with an increment of 0.01 e/Bohr^3.

Table 3 Calculated optical gap (in eV) for the CaF_2 bulk. Experimentally the direct band gap is 12.1 eV [1] and the indirect band gap is equal to 11.8 eV [2].

optical gap	LDA	PWGGA	PBE	BLYP	B3PW	B3LYP	HF
Γ–Γ	8.72	8.51	8.45	8.40	10.96	10.85	20.77
X–X	9.30	9.33	9.30	9.28	11.99	11.93	22.72
U–U	9.60	9.58	9.55	9.52	12.27	12.20	23.07
W–W	9.56	9.55	9.52	9.49	12.23	12.16	23.00
L–L	11.41	10.82	10.77	10.64	13.63	13.54	24.90
X–Γ	8.44	8.22	8.20	8.16	10.68	10.57	20.43
U–Γ	8.55	8.34	8.29	8.24	10.78	10.67	20.53
W–Γ	8.54	8.33	8.28	8.24	10.78	10.66	20.55
L–Γ	9.34	9.07	9.02	8.96	11.58	11.46	21.50

surface is collected in Table 4. Let us, for the analysis, look at the particular B3PW results, since they gave the best agreement with experiment for the lattice constant, bulk modulus and also the bulk band structure. The structure of $CaF_2(111)$ surface and directions of atomic displacements is illustrated in Fig. 4. The cation effective charges using the B3PW hybrid method in two top $CaF_2(111)$ surface layers (+1.797*e* and +1.802*e*) turn out to be smaller than in the bulk (+1.803*e*), whereas the F charges (–0.891*e*) in the upper sublayer of the top surface layer is by 0.011*e* larger as in the bulk (–0.902*e*). Changes in atomic charges in deeper layers become very small. Bond population analysis between atoms for the $CaF_2(111)$ surface shows, that the major effect observed here is the strengthening of the Ca–F chemical bond near the surface. Bond populations between Ca and F atoms in the upper sublayer of the first surface layer by (+12*me*) exceed the respective bond population value between Ca and F atoms in the bulk. At more deep layers of $CaF_2(111)$ surface, the bond population between Ca and F atoms is practically the same as in the bulk. The similar effect, strengthening of Ti–O chemical bond near the $SrTiO_3(001)$ surface, was observed by us before also for $SrTiO_3$ [22].

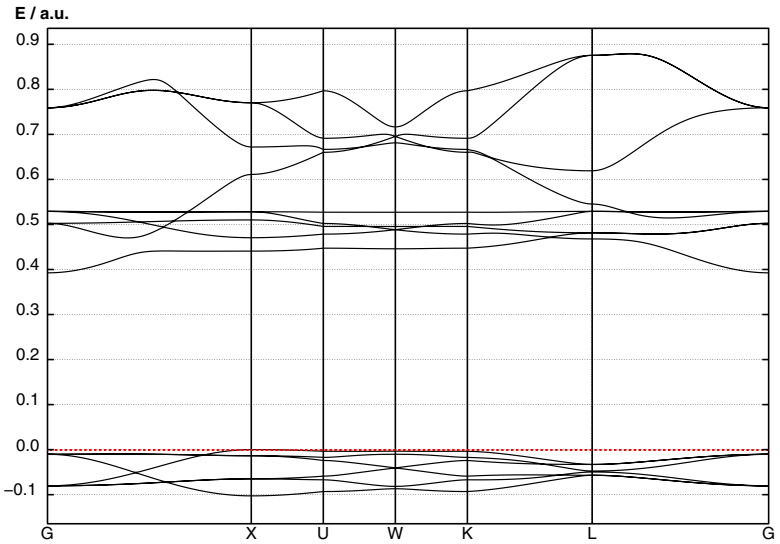

Fig. 2 (online colour at: www.pss-b.com) Electronic band structure of CaF_2 bulk calculated by means of the hybrid B3PW method.

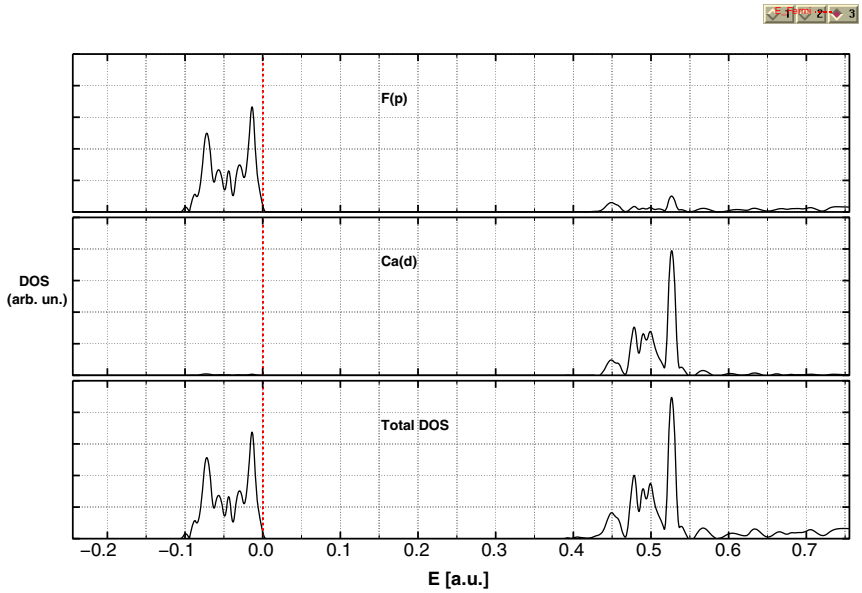

Fig. 3 (online colour at: www.pss-b.com) Calculated total and projected density of states (DOS) for CaF_2 bulk by means of hybrid B3PW method.

As a next step, we optimized the slab atomic structure for the case of $CaF_2(110)$ surface. We performed the geometry relaxation for the slab containing 15 layers (see Table 5). For $CaF_2(110)$ surface there appears an additional degree of freedom for atomic displacements in direction Y (see Fig. 5). Ca atom at $CaF_2(110)$ surface upper layer move inward (towards the bulk) by 3.35% of lattice constant a_0, whereas the displacement of upper layer Ca atom in the case of $CaF_2(111)$ termination was only 0.68% of a_0 towards the bulk. Also for more deep layers, the magnitudes of atomic displacements in the case of $CaF_2(110)$ surface is considerably larger as it is for $CaF_2(111)$ surface, see Tables 4 and 5 for comparison.

Table 4 Atomic relaxation of CaF_2 slab containing 9 layers in (111) direction (in percent of the lattice constant), calculated by means of hybrid B3PW method. Positive sign corresponds to outward atomic displacement (toward the vacuum).

layer	atom	B3PW Δz (%)
1	F	–0.90
	Ca	–0.68
	F	–0.78
2	F	–0.34
	Ca	–0.41
	F	–0.36
3	F	–0.34
	Ca	–0.28
	F	–0.23
4	F	–0.19
	Ca	–0.14
	F	–0.09
5	F	–0.05
	Ca	0
	F	0.05

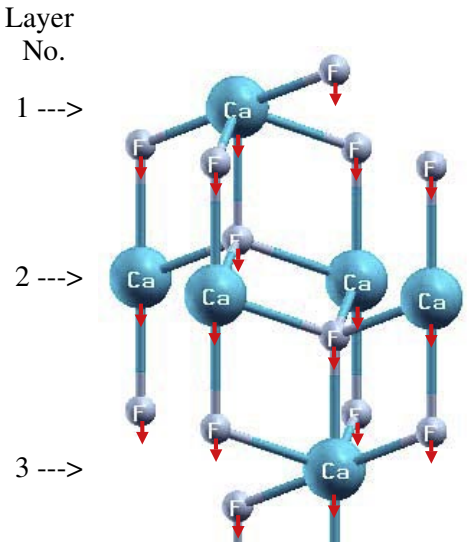

Fig. 4 (online colour at: www.pss-b.com) Schematic sketch of CaF_2(111) surface structure. Layer numbering introduced in this figure is used in Table 4. Arrows indicate the calculated displacement directions of Ca and F atoms.

The charge of the CaF_2(110) surface upper layer F atom is (–0.882e), and increases by 0.02e in comparison with bulk, and by 0.009e relatively to the CaF_2(111) surface upper layer F atom. The largest charge change is for the CaF_2(110) surface upper layer Ca atom. Its charge is reduced by –0.041e in comparison with the bulk charge (+1.803e) and equals to +1.762e. Charges in CaF_2(110) surface deeper layers becomes very close to the relevant Ca and F charges in the bulk.

Next, we calculated the relaxation of CaF_2(100) surface using the slab containing 15 layers (see Fig. 6). In order to get a stable and neutral CaF_2(100) surface we removed half of the F atoms from the F-terminated surface. We found, that relaxation of CaF_2(100) surface is considerably stronger as for (111) and (110) surfaces. F atoms at the upper surface layer is relaxed most noticeable, by 5.65% of a_0 towards the bulk, but also F atoms even at 7th layer are still considerably displaced, by 0.82% a_0 inwards and by 0.76% of lattice constant a_0 outwards (see Table 6).

Table 5 Atomic relaxation of CaF_2 slab containing 15 layers in (110) direction, calculated by means of hybrid B3PW method. Δy is the relative displacement (in percents of a_0) between two F atoms. Negative sign means shortening of the F-F distance.

layer	atom	B3PW, Δy (%)	B3PW, Δz (%)
1	F	+3.21	–0.87
	Ca	0	–3.35
2	F	–0.14	–0.83
	Ca	0	+0.80
3	F	+0.08	–0.26
	Ca	0	–0.88
4	F	–0.03	–0.40
	Ca	0	–0.13
5	F	+0.03	–0.22
	Ca	0	–0.33
6	F	–0.03	–0.18
	Ca	0	–0.13
7	F	+0.03	–0.08
	Ca	0	–0.09

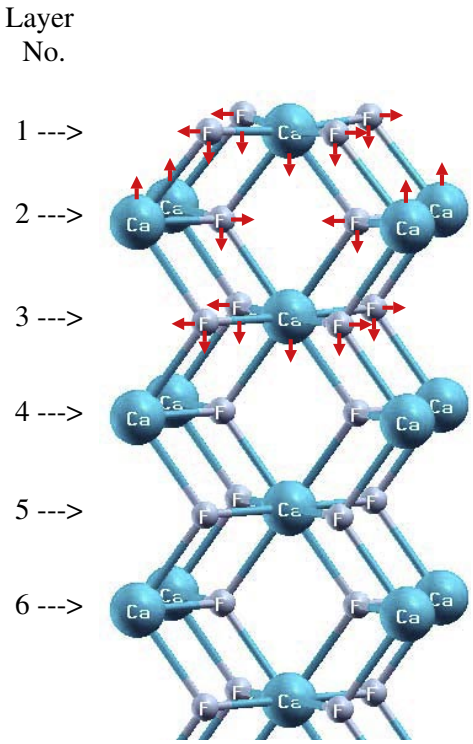

Fig. 5 (online colour at: www.pss-b.com) Schematic sketch of CaF_2(110) surface structure. For CaF_2 surface there appears an additional degree of freedom in direction Y for atomic displacements. Arrows indicate the calculated displacement directions of Ca and F atoms.

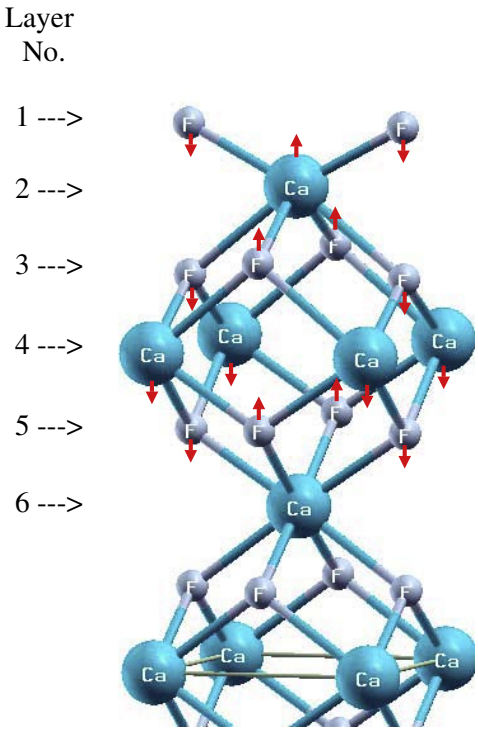

Fig. 6 (online colour at: www.pss-b.com) Schematic sketch of CaF_2(100) surface structure. Layer numbering introduced in this figure is used in Table 6. Arrows indicate the calculated displacement directions of Ca and F atoms.

Table 6 Atomic relaxation of CaF_2 slab containing 15 layers in (100) direction (in percent of the lattice constant), calculated by means of the hybrid B3PW method. Positive sign corresponds to outward atomic displacement (toward the vacuum).

layer	atom	B3PW, Δz (%)
1	F	–5.63
2	Ca	+0.34
3	F	–3.20
	F	+4.03
4	Ca	–0.03
5	F	+1.49
	F	–1.53
6	Ca	–0.07
7	F	–0.82
	F	+0.76

Static Mulliken charges of atoms for the $CaF_2(100)$ surface containing 15 layers calculated by the hybrid B3PW method differs from the bulk charges by +0.055*e* for the F and by –0.052*e* for the Ca, which is considerably more as in the cases of $CaF_2(110)$ and (111) surfaces. We can observe an increase of Ca–F bond population near the $CaF_2(100)$ surface by (+18*me*) in comparison with CaF_2 bulk and thereby a strengthening of Ca–F chemical bonding. The strengthening of Ca–F chemical bonding between Ca and F atoms in the upper surface layer is more pronounced for the $CaF_2(100)$ surfaces as it was for the $CaF_2(111)$ termination.

We computed also electronic energy band structure for $CaF_2(100)$, (110) and (111) surfaces using B3PW method. As we can see from the main results collected in Table 7, the direct optical band gap for the (111) surface (10.87 eV) is close to the relevant optical band gap value for the CaF_2 bulk (10.96 eV). The direct optical band gaps for $CaF_2(100)$ and (110) surfaces (9.95 eV and 10.13 eV) is considerably reduced in comparison to the CaF_2 bulk.

The calculated density of states (DOS) for the $CaF_2(100)$ surface shows, that the (100) surface upper layer F(p) orbitals moves upwards, towards the Fermi energy, with respect to the F(p) orbitals at more deep levels, and this leads to the narrowing of the (100) surface band gap from 10.96 eV for the case of CaF_2 bulk till 9.95 eV for the $CaF_2(100)$ surface. This finding is in line with the narrowing of the band gap at $SrTiO_3$, $BaTiO_3$, and $PbTiO_3$ perovskite (100) surfaces reported by us in Refs. [22–24] and by Padilla and Vanderbilt for $SrTiO_3$ and $BaTiO_3$ [25, 26] (100) surfaces. With increasing number of layers, the DOS for $CaF_2(100)$ surface gradually approaches that of bulk CaF_2.

Calculated DOS for the $CaF_2(110)$ surface shows that the (110) surfaces first layer F(p) atomic orbitals have some states near the Fermi energy, but their magnitudes is rather small. Thereby they contribute to some narrowing of the band gap, but this effect is not so well pronounced as in the case of $CaF_2(100)$ surface. The calculated optical band gap for $CaF_2(110)$ surface is 10.13 eV.

From calculated DOS for the $CaF_2(111)$ surface we can conclude, that the F(p) atomic orbitals in the upper layer of $CaF_2(111)$ surface have one large peak near the Fermi energy, whereas the F(p) DOS have two peaks at deeper layers, and with growing number of layers, they become more and more close to the

Table 7 Calculated direct ($\Gamma \rightarrow \Gamma$) optical gap (in eV) for the CaF_2 (100), (110) and (111) slabs. All calculations have been performed using hybrid B3PW method. The last column contains the respective optical gap for the CaF_2 bulk.

CaF_2 slabs	(100)	(110)	(111)	CaF_2 bulk
direct ($\Gamma \rightarrow \Gamma$) optical gap	9.95	10.13	10.87	10.96

Table 8 Surface energies for CaF_2 (111), (110) and (100) surfaces.

CaF_2 slabs	surface energies (J/m^2) this paper	surface energies (J/m^2) calculated in Ref. [9]	surface energy (J/m^2) experiment, Ref. [27]
(111)			
9 layers	0.438	0.467	0.45
7 layers	0.437	0.467	
(110)			
15 layers	0.719	0.819	
9 layers	0.717	0.819	
(100)			
15 layers	0.979	1.189	
9 layers	0.957	1.189	

relevant F(p) DOS for the CaF_2 bulk. The direct band gap value for the CaF_2(111) terminated surface (10.87 eV) is close to the bulk value of (10.96 eV).

3.3 Surface energies

We discuss next the surface energetics. The surface energy was calculated as

$$E_{\text{surface}} = \tfrac{1}{2}\left[E_{\text{slab}}^{(\text{relax})} - nE_{\text{bulk}} \right] \tag{1}$$

where n is the number of bulk primitive cells in the slab. E_{bulk} is the total energy per bulk unit cell, and $E_{\text{slab}}^{(\text{relax})}$ is the total energy for a relaxed slab containing n layers. Our calculated surface energies for CaF_2 (111), (110) and (100) surfaces containing different number of layers, using the hybrid B3PW functional are collected in Table 8. As we can see from results of our calculations, the (111) surface energy is the lowest (0.437 J/m^2) for the slab containing 7 layers, and practically do not depend on the number of layers in the slab. For the slab containing 9 layers, according to our calculations, the surface energy is practically the same (0.438 J/m^2). The calculated (111) surface energy, is very close to the (111) surface energy calculated earlier by Puchin et al. [9] (0.467 J/m^2), using the *ab initio* Hartree–Fock method, and in a good agreement with the only experimental estimation to our knowledge available (0.45 J/m^2) [27].

Our calculated surface energy for the (110) surface is considerably larger (0.719 J/m^2) as for (111) surface, and differs approximatelly by 12% from the (110) surface energy (0.819 J/m^2) calculated in Ref. [9].

Finally, our calculations show, that the surface energy for the (100) surface is the largest one (0.979 J/m^2) and is in a qualitative agreement with the result of previous *ab initio* (HF) calculation mentioned in Ref. [9] (1.189 J/m^2). As we can see from our results, obtained with the hybrid B3PW method, the surface energy for the (111) surface (0.437 J/m^2) is the lowest one, in comparisson with the (110) and (100) surfaces, thereby indicating, that the (111) surface is the most stable, in agreement with the experiment.

4 Conclusions

Summing up, a comparison of *ab initio* HF and DFT calculations employing different exchange-correlation functionals clearly demonstrates that the best agreement with experiment for the lattice constant, bulk modulus and as well as the band structure is possible to achieve by the hybrid B3PW functional. *Ab initio* HF method overestimates the band gap by factor of two, whereas our DFT calculations considerably underestimates it. According to our calculations, using the hybrid B3PW method, the direct band gap for the CaF_2 bulk (10.96 eV) is narrowed for the (111) (10.87 eV), (110) (10.13 eV) and (100) (9.95 eV) surfaces. The CaF_2 surface energy, according to our calculations is the smallest one

(0.437 J/m^2), indicating that the (111) surface is the most stable, in a good agreement with results of previous theoretical simulations, as well as the only, to our knowledge, available experimental result.

Acknowledgements The present work was supported by NATO CLG 980378 Grant and Deutsche Forschungsgemeinschaft (DFG).

References

[1] M. Verstraete and X. Gonze, Phys. Rev. B **68**, 195123 (2003).
[2] G. W. Rubloff, Phys. Rev. B **5**, 662 (1972).
[3] J. Barth, R. L. Johnson, M. Cardona, D. Fuchs, and A. M. Bradshaw, Phys. Rev. B **41**, 3291 (1990).
[4] F. Gan, Y. Xu, M. Juang, and W. Y. Ching, Phys. Rev. B **45**, 8248 (1992).
[5] W. Y. Chiang, F. Gan, and M. Huang, Phys. Rev. B **52**, 1596 (1995).
[6] M. Catti, R. Dovesi, A. Pavese, and V. R. Saunders, J. Phys.: Condens. Matter **3**, 4151 (1991).
[7] A. S. Foster, C. Barth, A. L. Shluger, R. M. Nieminen, and M. Reichling, Phys. Rev. B **66**, 235417 (2002).
[8] A. Jockisch, U. Schröder, F. W. Wette, and W. Kress, J. Phys.: Condens. Matter **5**, 5401 (1993).
[9] V. E. Puchin, A. V. Puchina, M. Huising, and M. Reichling, J. Phys.: Condens. Matter **13**, 5401 (1993).
[10] M. Merawa, M. Lunell, R. Orlando, M. Gelize-Duvignau, and R. Dovesi, Chem. Phys. Lett. **368**, 7 (1998).
[11] A. V. Puchina, V. E. Puchin, E. A. Kotomin, and M. Reichling, Solid State Commun. **106**, 285 (1998).
[12] R. W. G. Wyckoff, Crystal Structures, 9th ed. (Interscience/John Wiley, New York, 1963), Vol. 1.
[13] P. Camy, J. L. Doualan, S. Renard, A. Braud, V. Menard, and R. Moncorge, Opt. Commun. **236**, 395 (2004).
[14] G. A. Kumar, R. Riman, S. C. Chae, Y. N. Yang, I. K. Bae, and H. S. Moon, J. Appl. Phys. **95**, 3243 (2004).
[15] T. Tsujibayashi, K. Toyoda, S. Sakuragi, M. Kamada, and M. Itoh, Appl. Phys. Lett. **80**, 2883 (2002).
[16] V. R. Saunders, R. Dovesi, C. Roetti, M. Causa, N. M. Harrison, R. Orlando, and C. M. Zicovich-Wilson, CRYSTAL-2003 User Manual, University of Torino, Italy (2003).
[17] M. Causa and A. Zupan, Chem. Phys. Lett. **220,** 145 (1994).
[18] H. B. Schlegel, J. Comput. Chem. **3**, 214 (1982).
[19] B. Civalleri, P. D'Arco, R. Orlando, V. R. Saunders, and R. Dovesi, Chem. Phys. Lett. **348**, 131 (2001).
[20] C. Pisani (ed.), Quantum-Mechanical Ab-initio Calculations of the Properties of Crystalline Materials, Vol. 67 of Lecture Notes in Chemistry (Springer, Berlin, 1996).
[21] J. Muscat, A. Wander, and N. M. Harrison, Chem. Phys. Lett. **342**, 397 (2001).
[22] E. Heifets, R. I. Eglitis, E. A. Kotomin, J. Maier, and G. Borstel, Phys. Rev. B **64**, 235417 (2001).
[23] E. Heifets, R. I. Eglitis, E. A. Kotomin, J. Maier, and G. Borstel, Surf. Sci. **513**, 211 (2002).
[24] R. I. Eglitis, S. Piskunov, E. Heifets, E. A. Kotomin, and G. Borstel, Ceram. Int. **30**, 1989 (2004).
[25] J. Padilla and D. Vanderbilt, Surf. Sci. **418**, 64 (1998).
[26] J. Padilla and D. Vanderbilt, Phys. Rev. B **56**, 1625 (1997).
[27] J. J. Gilman, J. Appl. Phys. **31**, 2208 (1960).